

Biocompatible magnetic fluids: a comparative birefringence investigation

P.P. Gravina^a, J.S. Santos^a, L.C. Figueiredo^a, K. Skeff Neto^{a,b}, M.F. Da Silva^a,
N. Buske^c, C. Gansau^c, P.C. Morais^{a,*}

^a *Universidade de Brasília, Instituto de Física, Núcleo de Física Aplicada, 70919-970 Brasília-DF, Brazil*

^b *FINATEC, 70910-900 Brasília-DF, Brazil*

^c *Berlin Heart AG, Wiesenweg 10, D-12247 Berlin, Germany*

Abstract

The static magnetic birefringence (SMB) of magnetite-based magnetic fluids coated with dextran and dimercaptosuccinic acid was investigated using the recent model proposed by Skeff Neto et al. (J. Appl. Phys. 89 (2001) 3362). The SMB data of samples presenting particle concentration around 1.2×10^{16} particle/cm³ were successfully described. The particle size distribution obtained from the fit of the SMB data was discussed in comparison with the data obtained from transmission electron microscopy.

© 2002 Elsevier Science B.V. All rights reserved.

Keywords: Birefringence; Domains; Micromagnetism; Magnetic fluids; Magnetite; Permeability

In biocompatible magnetic fluids (BMFs) electrostatic plus steric repulsion may work together against colloidal instability. The most striking aspect of BMFs is the possibility that colloidal stability may be achieved at physiological pH and salinity. Adding non-toxicity to these features (pH and salinity), one has the basic ingredients of BMFs [1,2]. Biological specificity may be brought into BMFs, once a wide variety of bioactive molecules can be used to perform an extra coating on top of the first coating layer (pre-coating) of the magnetic nanoparticle [3]. Separation and purification of cells [4], drug delivery systems [5], contrast agents for magnetic resonance imaging [6], and hyperthermia of biological tissues applied to tumor therapy [7] are just a few examples of the many possibilities of applications of BMFs in biology and medical diagnosis and therapy. In hyperthermia, for instance, one seeks to achieve the highest magnetic response due to an applied modulation field, which in turn depends upon the magnetic susceptibility and magnetic moment of the existing magnetic structure.

Zero-field birefringence [8,9] as well as static magnetic birefringence (SMB) have been proved to be excellent tools in the investigation of the relative frequency of distinct magnetic structures in magnetic fluids. As long as the description of the SMB signal includes agglomerates and the particle size polydispersity, the field dependence of the magnetic susceptibility and the relative frequencies of monomer, dimer, trimer, and higher magnetic structures are obtained [10].

Magnetite nanoparticles used in this study were obtained by chemical co-precipitation of Fe (II) and Fe (III) ions in alkaline medium. After precipitation, the magnetite nanoparticle was surface-coated with two molecular agents, namely, dextran and dimercaptosuccinic acid (DMSA), respectively samples A and B, to produce stable BMF samples at physiological pH and salinity. BMF samples containing about 1.2×10^{16} particle/cm³ were used to perform the SMB measurements. Room temperature SMB data were obtained through the usual lock-in detection technique. The experimental setup consists of a chopped laser beam (632 nm) crossing perpendicularly the sample cell before illuminating the photodetector. The sample cell consists of a double goniometer-like device that allows full

*Corresponding author. Fax: +55-61-273655.

E-mail address: pcmor@unb.br (P.C. Morais).

angular rotation of both polarizer and analyzer and it is mounted in the gap of an electromagnet in such a way that the laser beam and the external magnetic field are perpendicular to one another [11].

Figs. 1(a) and (b) show the SMB data of samples A and B, respectively. Symbols represent experimental data while solid lines represent the best fit according to the model proposed in Ref. [10]. The model used to fit the SMB data is an extension of the model proposed by Xu and Ridler [12]. The extension of the Xu and Ridler model includes the field dependence of the magnetic permeability of the chainlike magnetic structures (dimers for instance). Shortly, the SMB signal ($\Delta\bar{n}$) description includes the diameter (D) lognormal distribution function, $P(D)$, plus the magnetization associated to monomer and dimer, i.e.:

$$\Delta\bar{n}(H; \bar{D}_B, \sigma_B, \bar{H}_Q, \sigma_Q) = A \frac{\int_0^\infty \left[\sum_Q C_Q \Delta n_Q(H, D) D^3 P(D) dD \right]}{\int_0^\infty D^3 P(D) dD} \quad (1)$$

with

$$\Delta n_Q(H, D) = \left[1 - \frac{3}{\xi_Q} \coth(\xi_Q) + \frac{3}{\xi_Q^2} \right].$$

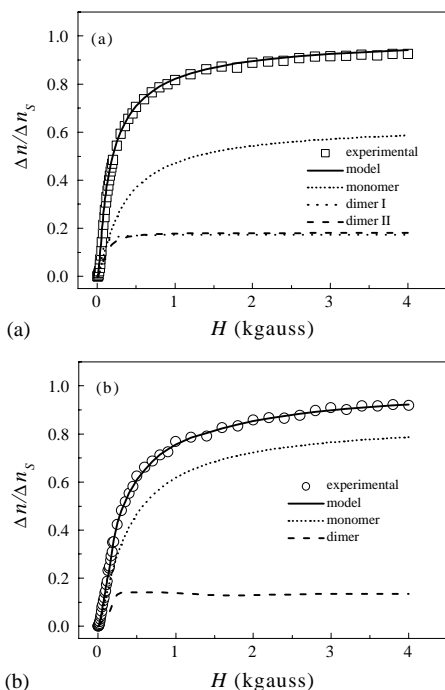


Fig. 1. Field dependence of the normalized SMB of (a) sample A and (b) sample B. Symbols are experimental data while solid lines are the best fit using Eq. (1). Broken lines represent the contributions from monomers and dimers.

The integral in Eq. (1) is carried out over $P(D)$, defined through a mean particle diameter (\bar{D}_B) and a standard deviation (σ_B), while the summation takes into account the particle aggregation with C_Q (fraction of magnetic structure Q) constrained by $\sum_{Q=1}^{\infty} C_Q = 1$.

The SMB data shown in Figs. 1(a) and (b) were best fitted assuming the presence of *monomers* (MM) and *dimers* (DM). $\xi_{MM} = (\pi/6)M_s D^3 H/kT$ accounts for monomer ($Q = 1$), while $\xi_{DM} = Q\xi_{MM}[1 + \beta C_{DM} F_{DM}(H)]$ describes the dimer contribution ($Q = 2$). M_s , k , T , and β are the saturation magnetization, the Boltzmann constant, the absolute temperature, and a constant, respectively. Note that the relative permeability (μ_{rel}) is given by $\mu_{rel} = 1 + \beta C_Q F_Q(H)$, where $F_Q(H)$ is the lognormal distribution function defined by a mean field (\bar{H}_Q) and a standard deviation (σ_Q) [13]. In Eq. (1) A is a constant related to the refractive index of the suspending medium, the number of particles, and the average optical anisotropy factor of the monomer.

Table 1 summarizes the main parameters obtained from the fit of the experimental data. Four aspects related to the data shown in Table 1 will be highlighted in what follows. First, the particle size polydispersity parameters obtained from the fitting of the SMB data ($\bar{D}_B = 9.4(9.4)$ nm and $\sigma_B = 0.29(0.27)$) are slightly different from the parameters obtained from the transmission electron microscopy (TEM) data ($\bar{D}_T = 9.4$ nm and $\sigma_T = 0.32$), as reported in Ref. [11]. The narrowing of the standard deviation $\sigma_B = 0.29(0.27)$ compared to $\sigma_T = 0.32$ has been attributed to the presence of small particles that do not make any contribution to the SMB signal [11]. Second, sample A has about 27% less monomers than sample B, though the core magnetite is the same. The difference would be explained based on the particle–particle interaction through the coating layer. While the dextran coating BMF (sample A) allows particle–particle interaction via hydrogen bonding, the DMSA coating BMF (sample B) may not. In other words, dimer formation is expected to be much more favorable in sample A than in sample B, as shown from the fitting of the SMB data (see Table 1).

Table 1

Some of the most relevant parameters obtained from the fit of the SMB data according to the model described by Eq. (1)

	Sample A	Sample B
\bar{D}_B (nm)	9.4	9.4
σ_B	0.29	0.27
C_1	0.63	0.86
C_2^I	0.18	—
C_2^{II}	0.19	0.14
\bar{H}_2^I (G)	277	—
\bar{H}_2^{II} (G)	670	475

Thus, the occurrence of two types of dimers (fanning and coherent) in sample A against just one type of dimer in sample B is straightforward. Finally, the relative permeability (μ_{rel}) associated to samples A and B peak at quite different values. While permeability in sample A peaks at two extreme values (277 and 670 G), permeability in sample B peaks at an intermediate value (475 G). Location of the permeability peak would be important in the design of magnetohyperthermia systems, once heat-generation could be enhanced for field modulation around permeability peaks.

In summary, the model presented in this study to analyze the SMB data, including the field dependence of the magnetic permeability, the particle size polydispersity, and the presence of monomers/dimers, was successfully used to explain the data obtained from BMF samples.

This work was partially supported by the Brazilian agencies FAP-DF, CNPq, FINATEC, and CAPES.

References

- [1] Z.G.M. Lacava, R.B. Azevedo, L.M. Lacava, E.V. Martins, V.A.P. Garcia, C.A. Rébola, A.P.C. Lemos, M.H. Sousa, F.A. Tourinho, P.C. Morais, M.F. Da Silva, *J. Magn. Magn. Mater.* 194 (1999) 90.
- [2] Z.G.M. Lacava, R.B. Azevedo, E.V. Martins, L.M. Lacava, M.L.L. Freitas, V.A.P. Garcia, C.A. Rébola, A.P.C. Lemos, M.H. Sousa, F.A. Tourinho, M.F. Da Silva, P.C. Morais, *J. Magn. Magn. Mater.* 201 (1999) 431.
- [3] A. Halbreich, J. Roger, J.N. Pons, M.F. Da Silva, E. Hasmonay, M. Roudier, M. Boynard, C. Sestier, A. Amri, D. Geldweth, B. Fertil, J.C. Bacri, D. Sabolovic, in: W. Schutt, J. Teller, U. Häfeli, M. Zborowski (Eds.), *Scientific and Clinical Applications of Magnetic Carriers*, Plenum Press, New York, 1997, p. 399.
- [4] P. Hermetin, R. Doenges, V. Franssen, C. Bieva, F.J.V. Bruggen, *Bioconjugate Chem.* 1 (1990) 411.
- [5] A. Kuznetsov, V.I. Filippov, O.A. Kuznetsov, V.G. Gerlivanov, E.K. Dobrinsky, S.I. Malashin, *J. Magn. Magn. Mater.* 194 (1999) 22.
- [6] C.W. Jung, J.M. Rogers, E.V. Groman, *J. Magn. Magn. Mater.* 194 (1999) 210.
- [7] A. Jordan, R. Scholz, P. Wust, H. Fhlingm, H. Felix, *J. Magn. Magn. Mater.* 201 (1999) 413.
- [8] A.F. Bakuzis, M.F. da Silva, P.C. Morais, K. Skeff Neto, *J. Appl. Phys.* 87 (2000) 2307.
- [9] A.F. Bakuzis, M.F. da Silva, P.C. Morais, L.S.F. Olavo, K. Skeff Neto, *J. Appl. Phys.* 87 (2000) 2497.
- [10] K. Skeff Neto, A.F. Bakuzis, P.C. Morais, A.R. Pereira, R.B. Azevedo, L.M. Lacava, Z.G.M. Lacava, *J. Appl. Phys.* 89 (2001) 3362.
- [11] B.M. Lacava, R.B. Azevedo, L.P. Silva, Z.G.M. Lacava, K. Skeff Neto, N. Buske, A.F. Bakuzis, P.C. Morais, *Appl. Phys. Lett.* 77 (2000) 1876.
- [12] M. Xu, P.J. Ridler, *J. Appl. Phys.* 82 (1997) 326.
- [13] C. Papusoi Jr., *J. Magn. Magn. Mater.* 195 (1999) 708.